

## Voltage Applicable to Au/YBa<sub>2</sub>Cu<sub>3</sub>O<sub>7</sub> Meander Lines

H.-R. Kim<sup>\*</sup>, S.-W. Yim, S.-D. Yu, C.-R. Park, S.-E. Yang, W.-S. Kim, and O.-B. Hyun

*Korea Electric Power Research Institute, Daejeon, Korea*

(Received 13 September 2010 revised or reviewed 18 October 2010 accepted 19 October 2010)

### Au/ YBa<sub>2</sub>Cu<sub>3</sub>O<sub>7</sub> 곡선에 인가가능 전압

김혜림<sup>\*</sup>, 임성우, 유승덕, 박충렬, 양성은, 김우석, 현옥배

#### Abstract

We investigated the voltage applicable to Au/YBa<sub>2</sub>Cu<sub>3</sub>O<sub>7</sub> (YBCO) meander lines. The meander line was fabricated by patterning Au/YBCO thin films grown on sapphire substrates by photolithography. It was subjected to simulated AC fault currents, and the resistance was measured and analyzed. The samples were immersed in liquid nitrogen during the experiment for effective cooling. The voltage applicable to the meander lines depended on the fault duration. Dependence was strong at short fault durations, and weak at long durations. When the voltage was plotted as a function of the fault duration on a log-log scale, data fell more or less on straight lines for all meander lines. In other words, the voltage applicable to Au/YBCO meander lines on sapphire substrates was inversely proportional to  $t^b$ , where  $t$  is the fault duration and  $b$  ranges from 0.4 to 0.5. The results were analyzed quantitatively with the concept of heat balance. Under adiabatic condition, the voltage is to be inversely proportional to  $t^{0.5}$  for all samples. Less value of  $b$  for some samples is thought to be due to cooling of the samples by liquid nitrogen.

*Keywords* : quench, Au/YBCO thin films, rated voltage, heat balance, superconducting fault current limiter

#### I. Introduction

The superconducting fault current limiters (SFCL) is a promising solution against the fault current problem, because it can limit the fault current in a few milliseconds, insert high resistance into the circuit, and return to the normal operation state automatically once faults are removed. For this

reason there has been active research going on SFCLs [1-4]. In particular, the hybrid-type SFCL sped up the commercial application of SFCLs by improving economical feasibility. In the hybrid-type SFCL, the superconductor in the main circuit detects the fault current, a high-speed switch then commutates the current into a parallel circuit, and a reactor or resistor in the parallel circuit limits the fault current [5]. Since the fault current flows in the superconductor only for a short time, much less amount of superconductors are needed to build a

---

<sup>\*</sup>Corresponding author. Fax : +82-42-865-5904  
e-mail : hrkim@kepri.re.kr

hybrid-type SFCL. This reduces the cost of building an SFCL as well as of operating it.

Knowledge on quench properties of superconductors is important for the research and development of SFCLs because quench properties determine their performances. In particular, information on the voltage applicable to superconductors is needed in estimating the amount of the superconductor needed to build an SFCL. In this work, we investigated the voltage applicable to Au/YBa<sub>2</sub>Cu<sub>3</sub>O<sub>7</sub> (YBCO) meander lines on sapphire substrates. Resistance of the meander lines was measured at various applied voltages, and analyzed. The results were interpreted in terms of heat balance.

## II. Experimental details

The samples were fabricated based on 300 nm thick YBCO films grown on sapphire substrates of two- or four-inch diameter. The films were purchased from Theva in Germany. The critical current density of the films was around 3.0 MA/cm<sup>2</sup> and uniform within 5 %. The film was coated in-situ with a gold shunt layer. Thickness of the gold layer was 200 nm, and the deviation in thickness is small enough not to affect the quench distribution. The contact resistance between the Au layer and the YBCO films was negligible compared with the resistance of the Au layer. The film was patterned into a meander line of 3 mm width for four-inch diameter films and of 2 mm width for two-inch films by photolithography (Fig. 1).

Resistance of the Au/YBCO meander lines was measured using a fault simulation circuit (Fig. 2). The meander line was connected to the circuit, and an AC power supply,  $V_0$ , was used as the voltage source.  $R_0$  in the circuit stands for the line resistance. The fault was simulated by closing a switch  $S_1$  connected across the load, and cut off with a switch  $S_2$  several cycles after the fault so that the sample would not be subjected to fault currents for unnecessarily long time. Voltages and currents were measured simultaneously with a multi-channel data

acquisition system. During the measurement, the samples were immersed in liquid nitrogen for effective cooling.

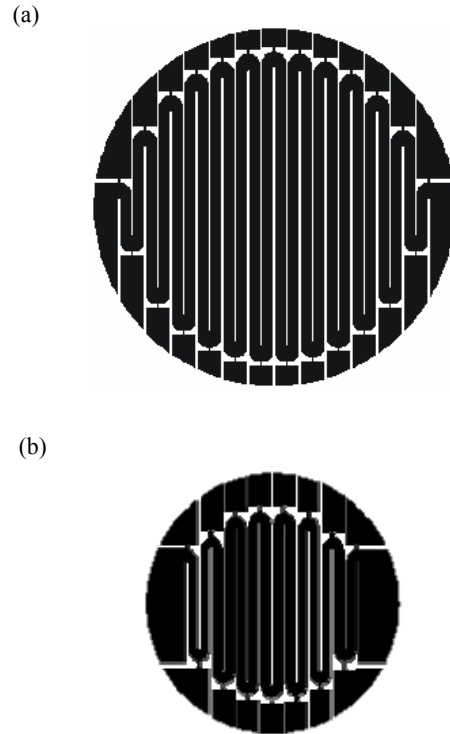


Fig. 1. The pattern of Au/YBCO meander lines (a) on a 4 inch-diameter substrate, and (b) on a 2 inch-diameter substrate. Not drawn to scale.

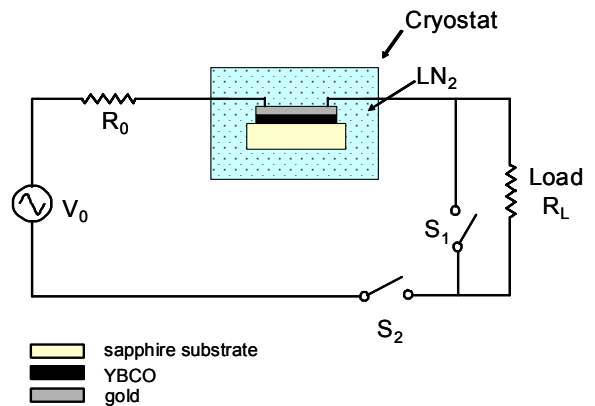


Fig. 2. A schematic diagram of the resistance measurement circuit.

III. Results and discussion

Fig. 3 shows resistance and current in an Au/YBCO meander line on a sapphire substrate of 4 inch diameter at applied voltage of 1 kV. Horizontal lines indicate resistance at selected temperatures of the meander line. Temperatures were estimated from data of resistance measured as a function of temperature on the meander line in the normal state. Resistance of Au/YBCO generally changes linearly with the temperature. The resistance increased rapidly at the beginning of the fault, and then slowly. It reached the values corresponding to meander line temperatures of 200 K, 250 K, and 300 K at around 17 ms, 40 ms, and 75 ms after the fault start, respectively. If maximum allowed temperature for the meander line is set to be 250 K, this result means that, when the fault duration is around 40 ms, the voltage applicable to the meander line is 1 kV.

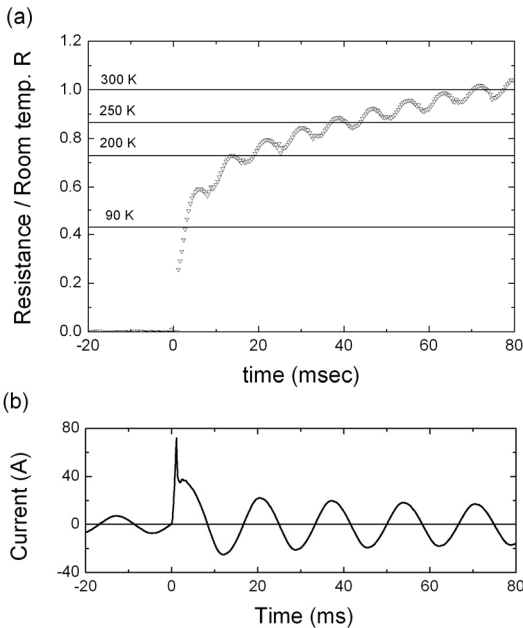


Fig. 3. (a) Resistance of, and (b) current in an Au/YBCO meander line during the fault at applied voltage of 1 kV.

Resistance during the fault of the same Au/YBCO meander line was measured at different applied voltages, and shown in Fig. 4(a). As the applied

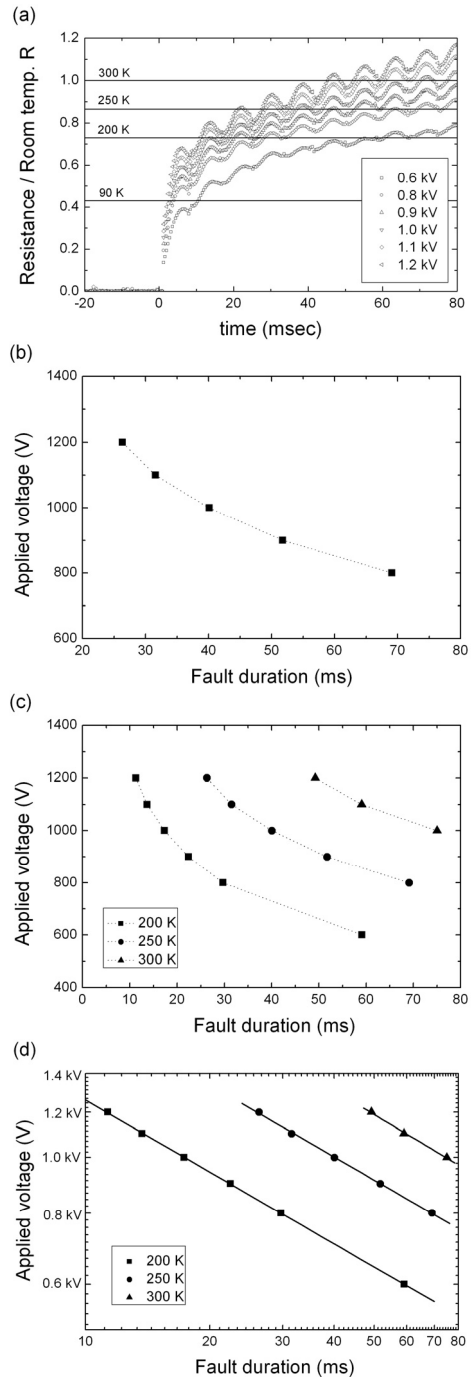


Fig. 4. (a) Resistance of an Au/YBCO meander line of 4 inch diameter during the fault at selected applied voltages, and the applied voltage as a function of time taken to reach (b) 250 K, (c) 200 K, 250 K and 300 K. (d) is a log-log plot of (c).

voltages were increased, the resistance increased in a similar manner, but faster, as expected. It took less time to reach 250 K at higher applied voltages, which means that higher voltage is applicable to the meander line for shorter faults. In order to quantify this, the applied voltage is plotted as a function of time taken for the temperature to reach 250 K in Fig. 4(b). Equivalently, the figure shows the voltage applicable to the meander line as a function of fault duration. The applicable voltage decreased with fault duration monotonously, somewhat faster for shorter durations and slower for longer durations. Shown in Fig. 4(c) is the applied voltage as a function of time taken to reach 200 K, 250 K and 300 K. It behaved similarly. When they were plotted on a log-log scale, data fell more or less on straight lines (Fig. 4(d)). The lines in the figure are linear fits to data points. That means that the voltage can be expressed in a power form:

$$V_0 = at^{-b}, \text{ where } a \text{ and } b \text{ are constants.} \quad (1)$$

*b*, the slope of the lines in Fig. 4(d), is about 0.42.

Fig. 5(a) shows resistance of another Au/YBCO meander line of 4 inch diameter at selected applied voltages. As the applied voltages were increased, the resistance increased faster, as above. The applied a voltage plotted as a function of time taken for the resistance to reach selected values is shown in Fig. 5(b). Again, the voltage decreased with fault duration monotonously, somewhat faster for shorter durations and slower for longer durations. When they were plotted on a log-log scale, data fell on straight lines again (Fig. 5(c)). The slope of the line that best fits the data was about 0.51 this time

Experiment was also carried out on Au/YBCO meander lines of 2 inch diameter (Fig. 1(b)). Fig. 6(a) shows resistance of the meander line at selected applied voltages. As the applied voltages were increased, the resistance increased faster, as for the meander lines of 4 inch diameter. The applied voltage was plotted as a function of time taken for the resistance to reach selected values on a log-log scale (Fig. 6(b)). Data fell on straight lines again, and

the slope of the line that best fits the data was about 0.41.

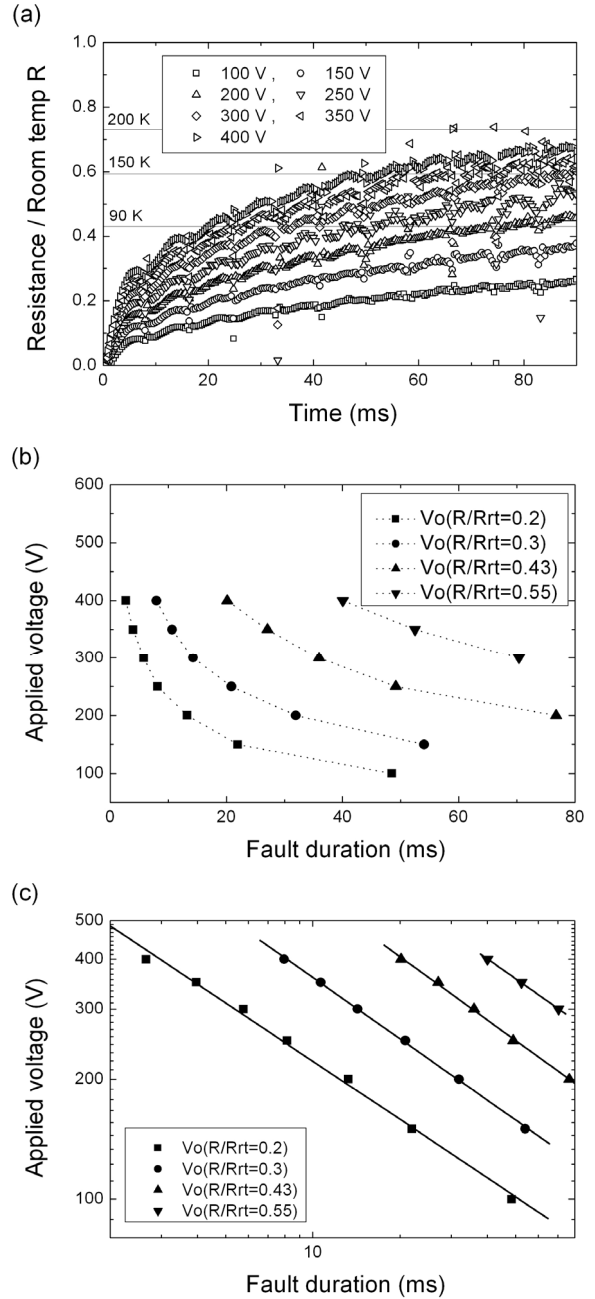


Fig. 5. (a) Resistance of another Au/YBCO meander line of 4 inch diameter during the fault, and (b) the applied voltage as a function of time taken to reach selected resistance. (c) is a log-log plot of (b).

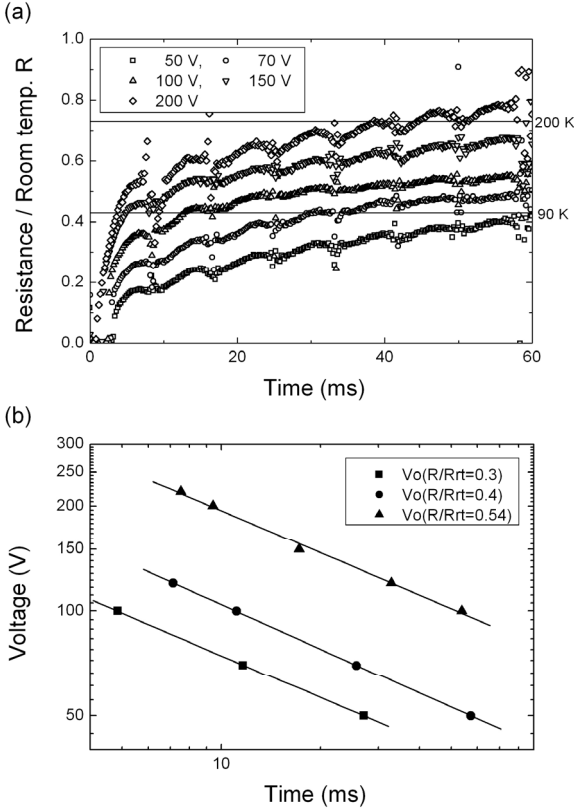


Fig. 6. (a) Resistance of an Au/YBCO meander line of 2 inch diameter during the fault, and (b) the applied voltage as a function of time taken to reach selected resistance on a log-log scale.

Thus, when the applied voltage was plotted as a function of time taken for the resistance to reach selected values on a log-log scale, data fell more or less on straight lines for all Au/YBCO meander lines. The slope of the line that best fits the data ranged from 0.4 to 0.5. This behavior of the meander-line resistance could be quantitatively explained in terms of heat balance. A part of the heat generated in the meander-lines during quenches increased their temperature, and the rest was transferred to surroundings. A heat balance equation describes this in a mathematical form:

$$c \frac{\partial T'}{\partial t} + \{\alpha \delta(z) + \alpha' \delta(z+d)\} T' - \kappa \nabla^2 T' = p, \quad (2)$$

where  $T' = T - T_b$ .

Here,  $c$ ,  $\alpha$ ,  $\alpha'$ ,  $d$ ,  $\kappa$ ,  $T_b$ , and  $p$  are specific heat, coefficient of heat transfer per unit area from the front and the back sides to surroundings, thickness of the sample, thermal conductivity, heat bath temperature, and density of power dissipated in the meander line during quenches, respectively. Terms on the left-hand side describe the heat that increases the sample temperature (the first term), and the heat transferred from the sample to surroundings and neighboring parts (the second and the third terms).

In our previous work [6, 7], it was observed that the temperature of the meander line was uniform in the thickness direction up to around 200 K and uniform also in xy direction except near the edge (around 3 mm from the edge) of the sample. Lower resistance at the edge was due to cooling by liquid nitrogen. Integrating (2) over the volume of the sample leads to:

$$C \frac{\partial T'}{\partial t} + S(\alpha + \alpha') T' - \kappa d \int \nabla_{xy}^2 T' dx dy = P, \quad (3)$$

where  $C$ ,  $S$  and  $P$  are heat capacity, surface area of the sample, and power dissipated in the sample, respectively.

$P = \int p dx dy dz$ . Since the temperature of the meander line was uniform in the thickness direction up to around 200 K,  $P$  can be expressed as

$$P = \{V_0 / (R + R_0)\}^2 R, \quad (4)$$

where  $R$ ,  $V_0$ , and  $R_0$  are resistance of the whole Au/YBCO meander line, the applied voltage, and the line resistance (Fig. 2), respectively. If it is assumed that cooling terms, the second and the third terms in the left hand side of (2), were negligible, (3) becomes:

$$C \frac{\partial T'}{\partial t} = \frac{V_0^2}{(R + R_0)^2} R \quad (5)$$

Re-arranging (5) and integrating leads to the following equation:

$$\int \frac{C(T')}{R(T')} (R(T') + R_0)^2 dT' = V_0^2 \int dt, \quad (6)$$

$$= V_0^2 t$$

This equation tells a great deal.  $C$  and  $R$  both depend on temperatures. But, however complex the dependence is, the left hand side of (6) is a number. In other words, for given sample, line impedance, and the temperature range, the left hand side of (6) is a constant, and hence  $V_0 \propto t^{-1/2}$ . In other words, the voltage that can be applied to the meander lines is proportional to  $t^{-1/2}$ . This coincides well with the experimental results shown in Fig. 5, and roughly with those shown in Figs. 4 and 6. Slight discrepancy between the latter and (6) is thought to be due to neglecting cooling terms in (3).

#### IV. Conclusions

We investigated the voltage applicable to Au/YBCO meander lines on sapphire substrates. The voltage depended on the fault duration. It decreased fast at shorter fault durations, and slowly at longer short durations. When the voltage was plotted as a function of the fault duration on a log-log scale, data fell more or less on straight lines for all meander lines. The slope of the line that best fits the data was in the range of 0.4 and 0.5. This means that the voltage applicable to Au/YBCO meander lines on sapphire substrates was inversely proportional to  $t^b$ , where  $t$  is the fault duration and  $b$  ranges from 0.4 to 0.5. The results were analyzed quantitatively with the concept of heat balance. Under adiabatic condition, the voltage is to be inversely proportional to  $t^{0.5}$  for all samples. Discrepancy in the value of  $b$  for some samples is thought to be due to neglecting cooling terms in the heat balance equation. These results will be applied to the design of SFCLs based on Au/YBCO meander lines on sapphire substrates, particularly to the design of the hybrid-type SFCLs.

#### Acknowledgments

This work was supported by a grant from the Power Generation and Electricity Delivery Program of the Korea Institute of Energy Technology Evaluation and Planning (KETEP) funded by the Korean government, Ministry of Knowledge Economy.

#### References

- [1] Mathias Noe and Michael Steurer, "High-temperature superconductor fault current limiters: concepts, applications, and development status", *Supercond. Sci. Tech.* 20, R15-R29 (2007)
- [2] H.-W. Neumueller, et al., "Development of resistive fault current limiters based on YBCO coated conductors", *IEEE Tr. Applied Supercond.* 19, 1950-1955 (2009)
- [3] T. Yazawa, et al., "Design and experimental results of three-phase superconducting fault current limiter using highly-resistive YBCO tapes", *IEEE Tr. Applied Supercond.* 19, 1956-1959 (2009)
- [4] J.-C. H. Llambes, D. W. Hazelton and C. S. Weber, "Recovery under load performance of 2nd generation HTS superconducting fault current limiter for electric power transmission lines", *IEEE Tr. Applied Supercond.* 19, 1968-1971 (2009)
- [5] Gyeong-Ho Lee, Kwon-Bae Park, Jungwook Sim, Young-Geun Kim, Il-Sung Oh, Ok-Bae Hyun, and Bang-Wook Lee, "Hybrid Superconducting Fault Current Limiter of the First Half Cycle Non-Limiting Type", *IEEE Tr. Applied Supercond.* 19, 1888-1891 (2009)
- [6] H.-R. Kim, J. Sim, O.-B. Hyun, "Temperature behavior of superconducting fault current limiters during quenches", *Progress in Superconductivity*, 6, 108-112 (2005)
- [7] Hye-Rim Kim, Ok-Bae Hyun, Hyo-Sang Choi, Sang-Do Cha, "Resistance distribution in a large area thin film type SFCLs", *J. Korea Inst. Applied Supercond. Cryogenics*, 4, 89-93 (2002)